Micro Area Analysis with JXA-8530F (FE-EPMA)

Norihisa Mori

SA Business Unit, JEOL Ltd.

The FE-EPMA, an electron probe micro analyzer (EPMA) equipped with a Schottky field emission (FE) electron gun, is designed to enhance the micro area analysis capability, achieving an analytical area of only 0.1 μm in size. Micro area analyses were studied on stainless steel and solder samples with a FE-EPMA to evaluate its spatial resolution, micro particle detection, and ability to quantify micro areas.

Introduction

FE-EPMA, an electron probe micro analyzer (EPMA) equipped with a Schottky field emission (FE) electron gun, is designed to enhance the microarea analysis capability [1], achieving an analytical area of the order of 0.1 μm across in size.

Typically the analytical area of EPMAs has been about 1 μm in both width and depth. The size of an analytical area is determined by the size of the electron probe at the surface and the spread of scattered electrons within the sample. At an accelerating voltage in the range of 15 to 20 kV, the range used most frequently in EPMA, the analytical area is principally determined by the area of electron scattering within the sample, which is typically around 1 μm in diameter.

At lower accelerating voltages, the analytical area is reduced because the electron scattering within the sample becomes smaller. However, it is also critical not to decrease the accelerating voltage during high spatial resolution analyses because the size of the electron probe becomes larger at lower accelerating voltages. In EPMAs with a tungsten filament, the horizontal spatial resolution does not improve significantly when the accelerating voltage is lowered to 15 kV or less. The use of a LaB_6 gun, with its ability to achieve a finer probe size, is effective for improving the horizontal spatial resolution, but only at accelerating voltages down to 10 kV.[2]

The EPMA can analyze almost all elements at accelerating voltages down to 6 kV, when the characteristic X-ray excitation voltage of all the X-ray lines are considered. Therefore, an EPMA with an FE gun, capable of achieving the finer probe at lower accelerating voltages and high probe currents needed for analysis, can improve the micro area analysis capability over the traditional EPMA with a tungsten or LaB_6 gun.

We have studied micro area analyses of stainless steel and solder samples with FE-EPMA to evaluate its performance in terms of spatial resolution, micro particle detection, and quantification of micro areas.

FE-EPMA(JXA-8530F)

JXA-8530F (**Fig.1**) is equipped with a high brightness Schottky field emission (FE) gun allowing an electron probe to focus on smaller areas than the conventional EPMA. The FE gun achieves a probe size 1/2 to 1/8 smaller when compared to the tungsten or LaB_6 gun. Alternatively, the FE gun can produce a probe current 20 to 100 times higher than the tungsten or LaB_6 gun with the same probe size (**Fig.2**).

An EPMA is commonly used with a probe current of 10 nA to 100 nA. We therefore compared the images of gold particles acquired with FE, LaB_6, and tungsten guns at an accelerating voltage of 10 kV and a probe current of 100 nA (**Fig. 3**). The results show

Fig. 1 JXA-8530F, EPMA with FE gun.

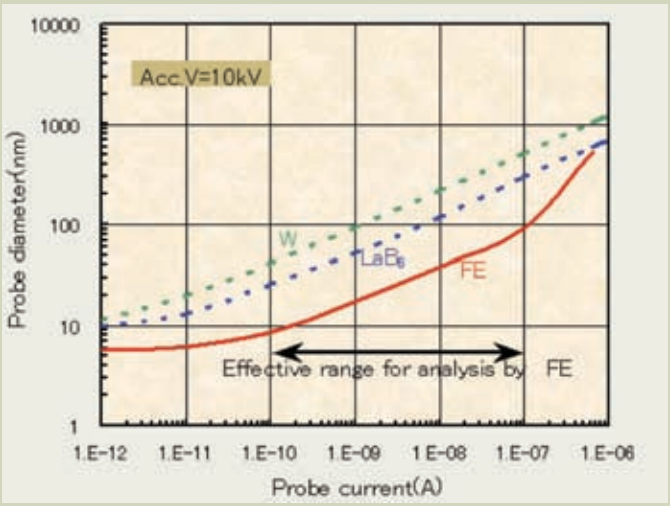

Fig. 2 Probe sizes achieved by JXA-8230 (W, LaB_6 guns) and JXA-8530F (FE gun).

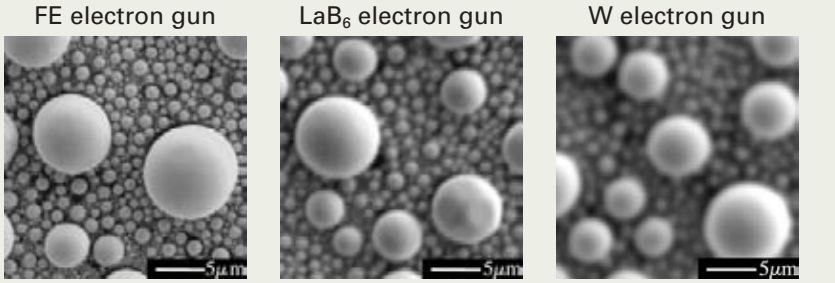

Fig. 3 Gold particles photographed with FE, LaB_6, and tungsten guns.
Conditions: Accelerating voltage 10 kV; probe current 100 nA.

that the FE gun, under conditions frequently used in actual analysis, is definitely superior to the LaB_6 or tungsten gun in terms of spatial resolution.

In addition to the electron gun, the JXA-8530F integrates various features that support high magnification analysis. It uses a two-stage differential pumping system to maintain the vacuum in the electron optics at an optimum level. This prevents changes in the vacuum in the specimen chamber from affecting the gun chamber, thereby achieving probe current stability needed for EPMA analysis. An optional liquid nitrogen trap, sustainable for 10 hours or longer, minimizes the re-absorption of residual gases in the specimen chamber or gases emitted from the sample, allowing samples that are susceptible to gas absorption to be analyzed overnight. Analyzing crystals for low energy X-ray analysis, such as the LDE series and TAPH, are also effective for enhancing the performance at low accelerating voltages.

Spatial resolution of X-ray mapping

To obtain X-ray maps with the highest spatial resolution, the probe size must be the smallest, and the accelerating voltage the lowest. If the accelerating voltage is higher, the area from which X-rays are generated becomes larger due to the electron scattering within the sample, thereby reducing the spatial resolution.

The W type EPMA needs to use a higher accelerating voltage (15 to 20 kV) to obtain the probe current needed for typical analysis, because it cannot achieve a small enough probe size at a lower accelerating voltage. The FE gun, however, can produce a probe size small enough for analysis at 10 kV or lower, achieving much higher spatial resolution.

A lead-free solder sample was analyzed at the same accelerating voltage (8 kV) with three different electron guns (**Fig. 4**). This

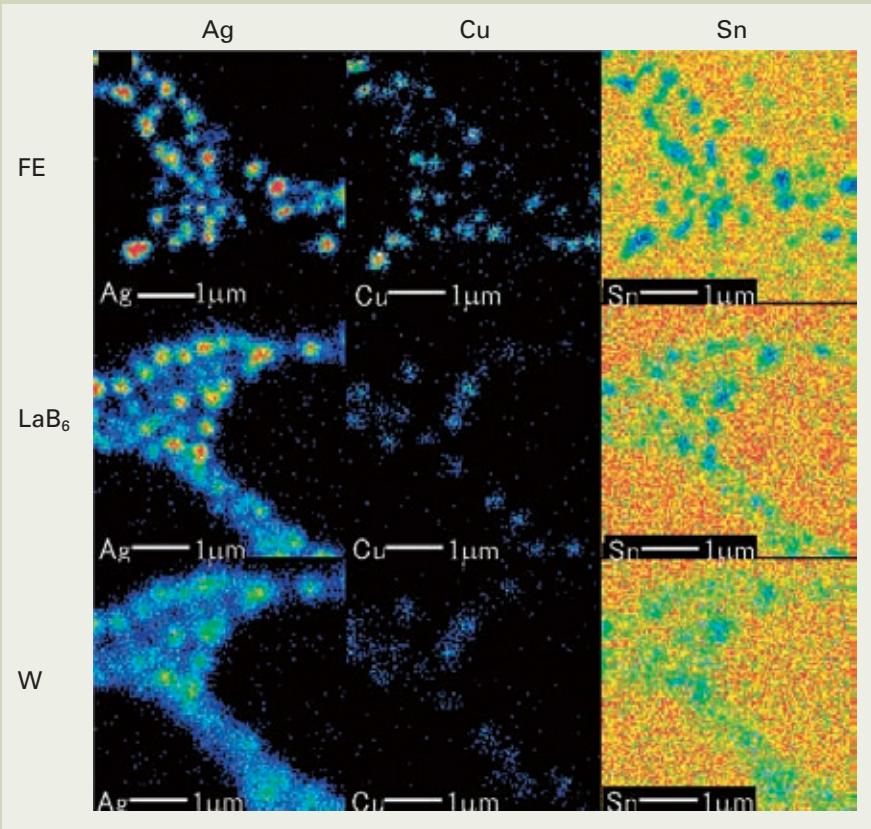

Fig. 4 X-ray images of Ag, Cu, and Sn in lead-free solder.
Conditions: Accelerating voltage 8 kV; probe current 10 nA.
The FE gun produced X-ray images with the highest spatial resolution. See attached color images.

lead-free solder contains numerous particles, that 1 μm or smaller in size, of either an Ag alloy or a Cu alloy distributed in the Sn matrix. The FE gun, with the smaller probe size, acquired the best X-ray maps with superior spatial resolution.

The spatial resolution of X-ray mapping of a bulk sample is considered to be around 0.1 μm when the FE gun is used at an accelerating voltage optimized for the probe size and the electron scattering within the sample. The appropriate accelerating voltage for the FE gun varies with different samples, but it ranging from 3 to 6 kV. The accelerating voltage should be lower for samples with a smaller mean atomic number, such as oxides. However, for samples with mean atomic number higher than Fe, the accelerating voltage should be set to 5 kV or 6 kV for optimum results.

Thus, the JXA-8530F, with its FE gun, can achieved a spatial resolution of around 0.1 μm by using a low accelerating voltage.

Detecting trace elements and micro particles

The results in the preceding section demonstrate that the JXA-8530F has a spatial resolution significantly better than the conventional EPMA. However, for elemental analyses, other systems are also widely used; those with similar capabilities to the EPMA (JXA-8230/8530F) include the FE-SEM+EDS (JSM-7001F), and those with higher spatial resolution include the AES (JAMP-9500F) and the TEM. The major difference between the EPMA and these other systems is that the EPMA uses wavelength dispersive X-ray spectrometer (WDS) for the elemental analysis. We will focus on two features below that sets WDS apart from the other techniques:

1) Superior detection of trace elements
2) Accurate quantitative analysis

Item (1) is related to the ability to detect micro particles, which is one of the critical factors in high-resolution analysis. Item (2) will be discussed in the next section.

Figure 5 is a backscattered electron image of stainless steel sample that contains Nb and C. Bright particles and extremely small particles with the size of 0.1 μm or less, are observed in the matrix. Nb and C maps of the stainless steel sample were collected by both WDS and EDS. **Figure 6** shows the results.

The remarkable difference between the WDS and EDS data can be seen in the distribution of particles in the carbon X-ray image. The WDS carbon X-ray image shows numerous small particles, whereas the EDS X-ray image hardly shows any of these particles. This demonstrates the difference in trace element detection between the WDS and the EDS capability.

Figure 7 illustrates how particles that are smaller than the analytical area of the EPMA are detected. Electron beam will scatter once they enter the sample. When the probe is placed onto a particle smaller than the analytical area, the beam will spread beyond the particle boundary. Since the particle size is smaller than the volume of the area being measured, the intensity of the measured X-rays will be lower.

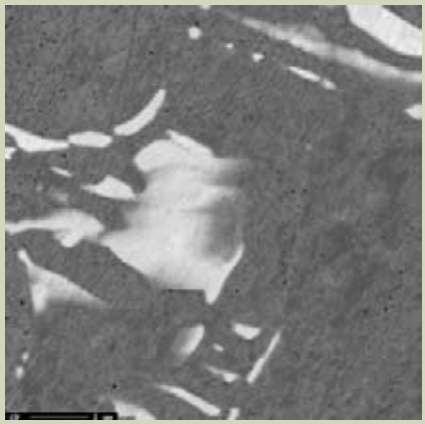

Fig. 5 BE composition image of stainless steel
Numerous black particles 0.1 μm or less present in matrix.

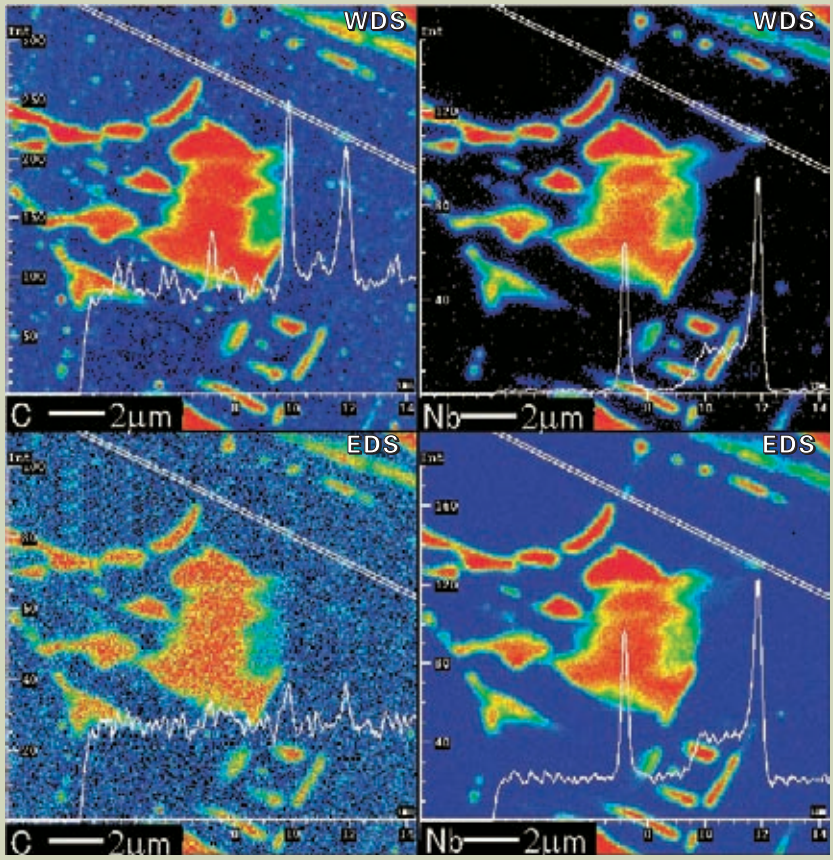

Fig. 6 WDS and EDS analysis of the area of view in Figure 5.
Line profile of straight line in each map.
Conditions: Accelerating voltage 7 kV; probe current 50 nA.

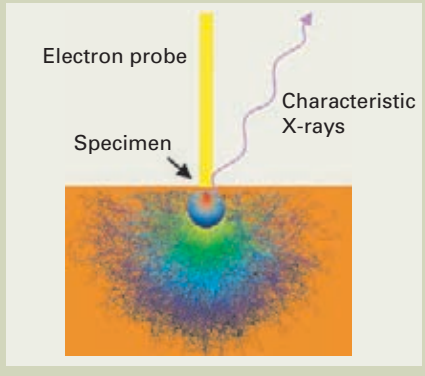

Fig. 7 The X-ray intensity is very low for particles 0.1 μm or smaller, due to the small volume from which these X-rays are being emitted.

	WDS	EDS
C	0.5%	2.7%
Nb	0.3%	1.0%

Fig. 8 Detection limits under mapping conditions used in Figure 6.

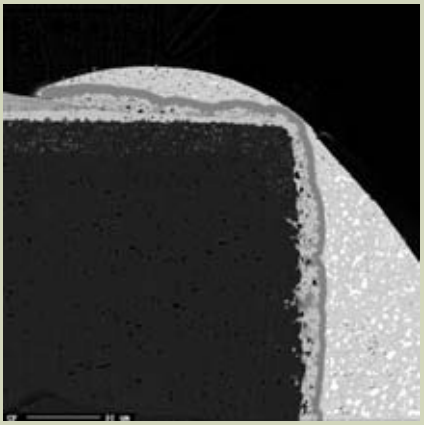

Fig. 9 BE composition image of chip resistor mounted to substrate (cross section).

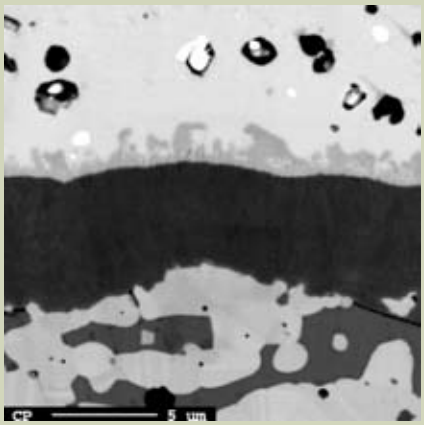

Fig. 10 Magnified image of Figure 9. Alloy layer present at the interface of Ni plating is at center and solder at top.

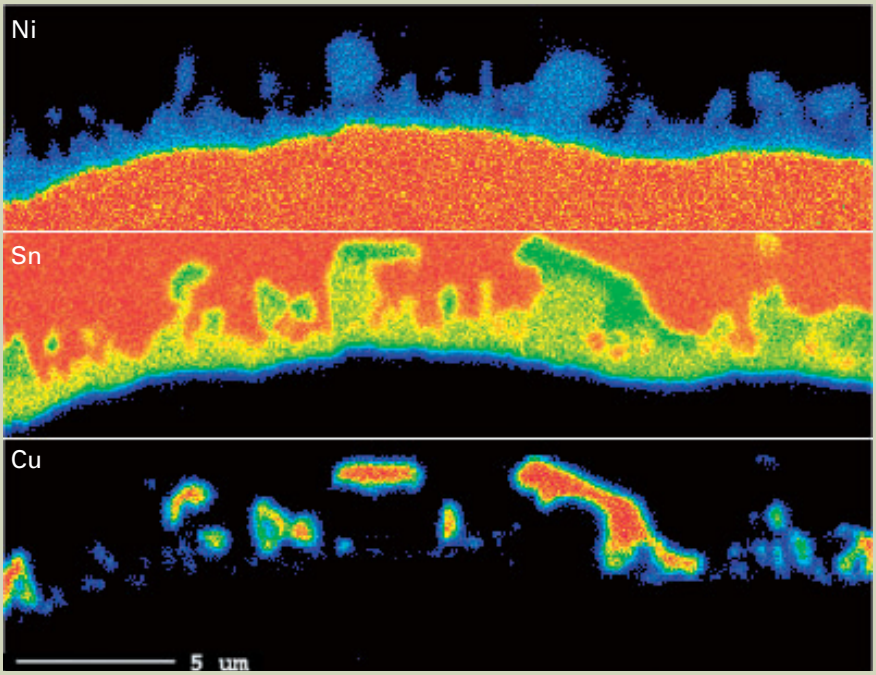

Fig. 11 X-ray image of the interface in Figure 10. Shown are NiSn and CuSn alloys distributed along the interface between Ni plating and solder.
Conditions: Accelerating voltage 6 kV; probe current 10 nA.

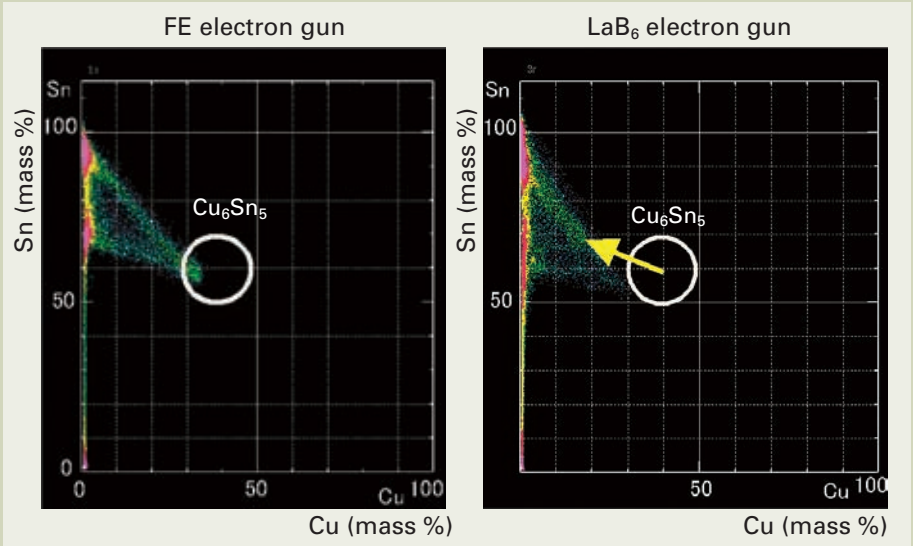

Fig. 12 Phase analysis of the area shown in Figure 11, comparing data acquired by FE and LaB_6 guns

This low X-ray intensity determines whether the trace elements are detectable. Therefore a system effective for analyzing trace elements is also best for analyzing micro particles. This applies to thin film analysis as well.

The detection limit of WDS or EDS is defined as follows:[3]

$$C_{DL} = \frac{3.29a}{\sqrt{\left(ntP\frac{P}{B}\right)}}$$

C_{DL} : Detection limit (mass %)
a : Correction coefficient (ZAF etc.)
n : Number of analytical spots
t : Measurement time (s)
P : Peak intensity of standard sample
P/B : P/B ratio of standard sample

The table (**Fig.8**) shows the results when the parameters for C and Nb are substituted in the formula above. The correction coefficient was assumed to be 1 for this example.

As the table shows, the ability of WDS to detect trace elements in mapping is higher than that for EDS. Thus, WDS is more effective in detecting micro particles than EDS.

AES and TEM systems have higher spatial resolution, but the location of particles is critical; particles must be either on the surface (AES) or inside a thin film (TEM). EPMA, on the other hand, can analyze particles containing trace elements that extend from the surface to a 0.1 to 1 µm depth within the sample by changing the accelerating voltage. The EPMA, with its wider range of analytical depths, is often better at detecting micro particles that exist within a sample than AES or TEM. Other examples of EPMA applications include studies of the distribution of Au scattered as micro particles in solder, and the detection of trace components, on the order of ppm, as impurities in stainless steels.

When WDS, effective for trace element detection as well as micro particle analysis, is combined with an FE gun, the result is a powerful analytical tool.

Spatial resolution in quantitative analysis

One advantage of WDS is its highly accurate quantitative analysis. A solder interface was selected as a test to determine the minimum size area capable of being quantitatively analyzed using WDS.

Figure 9 is a cross section of a chip resistor mounted to substrate. The interface between the Ni and the solder shown in the cross section was mapped. Results of this area analysis (**Fig. 11**) show that an Ni-Sn alloy layer occurs next to the Ni, Sn layer of solder is then in contact with the Ni-Sn alloy layer, and a Cu-Sn alloy layer occurs discontinuously between the Ni-Sn alloy and Sn layers. The Cu-Sn alloy layer is Cu_6Sn_5 which is a result of a Cu coating on the Ni surface that alloyed with the Sn.

Phase analysis was applied to the Cu_6Sn_5 alloy (**Figure 12**). The data from the area analysis were quantified and plotted, with the Sn mass concentration in the vertical axis and the Cu mass concentration in the horizontal axis.

When particles 0.2 µm in size are analyzed

at an accelerating voltage of 6 kV, approximately 10% of the X-rays will be emitted from outside of the particles, assuming a focused beam. Therefore, a circle with a radius of 10% was drawn at a point corresponding to the mass concentration of Cu_6Sn_5 on the scattered diagram, and it was assumed that the area within the circle was where the quantitative analysis was performed.

In the data obtained with the FE gun, numerous points occur within the area of the circle. Data obtained with the LaB_6 gun, shows very few points within the circle corresponding to Cu_6Sn_5, since higher Sn concentrations and lower Cu concentrations were measured due to the larger probe size that interacted with the Sn in the vicinity.

Phase analysis was carried out on another region to examine the Cu-Sn alloy distributed in layers at the interface between the solder and Cu (**Figs. 13** and **14**). The results show that in this sample, the thickness of the Cu_6Sn_5 alloy layer exceeds 1 μm. The data also shows another layer, 0.2 μm thick, at the interface between Cu and Cu_6Sn_5. This layer is a Cu_3Sn_1 alloy.

As before, a circle with a radius of 10% was drawn at each of the points corresponding to the mass concentrations of Cu_6Sn_5 and Cu_3Sn_1 on the scattered diagram. There is little difference between the in distribution of Cu_6Sn_5 data taken with the FE gun and the LaB_6 gun. However, for the 0.2 μm thick layer of Cu_3Sn_1 there are numerous points that plot within the circle in the FE gun data, while no apparent correlation was detected within the data from the LaB_6 gun. This demonstrates that the JXA-8530F can quantitatively analyze a layer only 0.2 μm thick. This is an area that is twice the size of the spatial resolution of X-ray imaging, which is 0.1 μm.

The X-ray emitting area spreads from the probe center. It is safe to assume that the area where 50% of the X-rays are emitted determines the spatial resolution. This has been verified by Monte Carlo simulation and actual measurements [2, 4].

For quantitative analysis where a 10% error is permitted, 90% of the X-rays emitted must come from the specific area being analyzed. The area where 90% of X-rays are emitted will be approximately twice the size of the area where 50% of X-rays are emitted. An area 3 times larger will include most of the X-rays that are emitted and will insure even more accurate quantitative results.

To summarize, the analysis of the solder interface by the JXA-8530F, demonstrates that the spatial resolution of X-ray imaging is about 0.1 μm, whereas for point analysis an area of 0.2 μm is required, if a 10% contribution from the matrix is acceptable, and 0.3 μm is required for high precision quantitative analysis.

Conclusion

The JXA-8530F with an FE gun was used for micro area analysis of stainless steel and solder samples to evaluate its spatial performance. The results of the bulk sample analyses at low accelerating voltage shows that the JXA-8530F is capable of:

1) Achieving a spatial resolution of 0.1 μm for X-ray imaging at low accelerating voltages;
2) Detecting micro particles even smaller than the defined spatial resolution using WDS effective for trace element detection;
3) Quantitative analysis of an area only 0.2 μm in size, subject to a 10% interference from the matrix; a higher accuracy is achieved with an area 0.3 μm in size.

References

[1] H. Yamada, T. Okumura, T. Kimura, W. Knoll, *Proc. of ICEM 15th DURBAN*, 343, (2002)

[2] N. Mori, *Proc. of The 19th International Congress on X-Ray Optics and Microanalysis (Kyoto, 2007)*, p34

[3] Joseph I. Goldstein, et. al Scanning Electron Microscopy and Xray Microanalysis, p 500, (1994)

[4] Ian Barkshire, Peter Karduck, Werner P. Rehbach, *Silivia Richter Mikrochim. Acta*, **132**, 113, (2000)

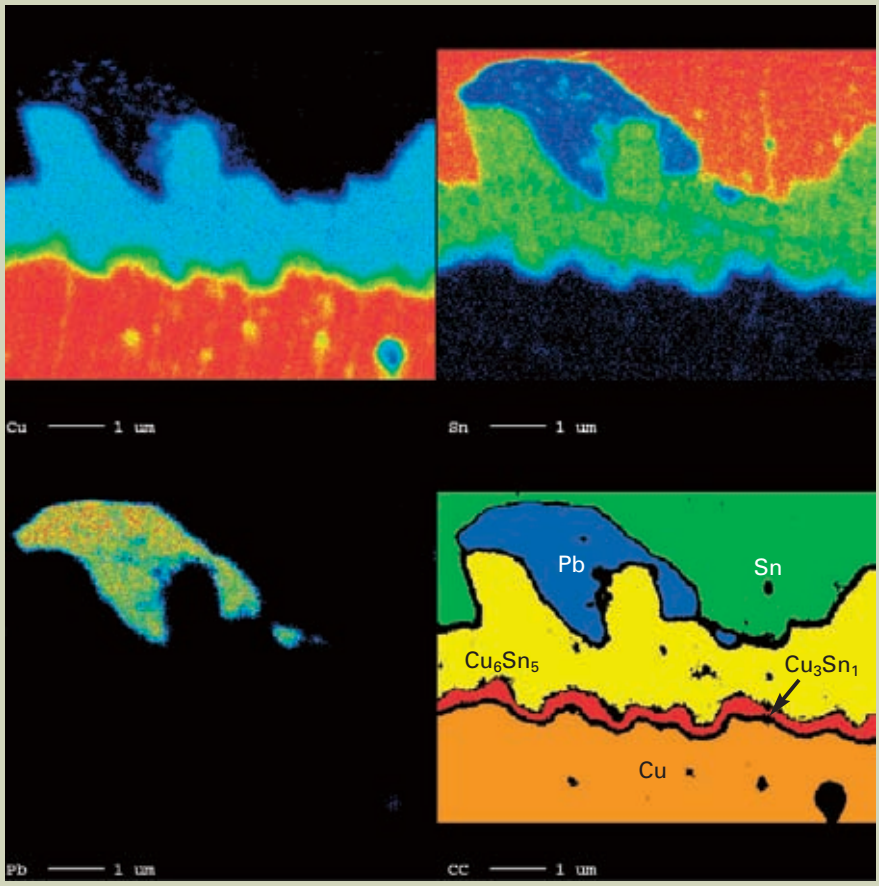

Fig. 13 X-ray image of the interface between solder and Cu. Cu_6Sn_5 and Cu_3Sn_1 alloys occur between the Sn and Cu. The image shows a Cu_3Sn_1 alloy layer 0.2 μm thick. See attached color images.
Conditions: Accelerating voltage 6 kV; probe current 10 nA.

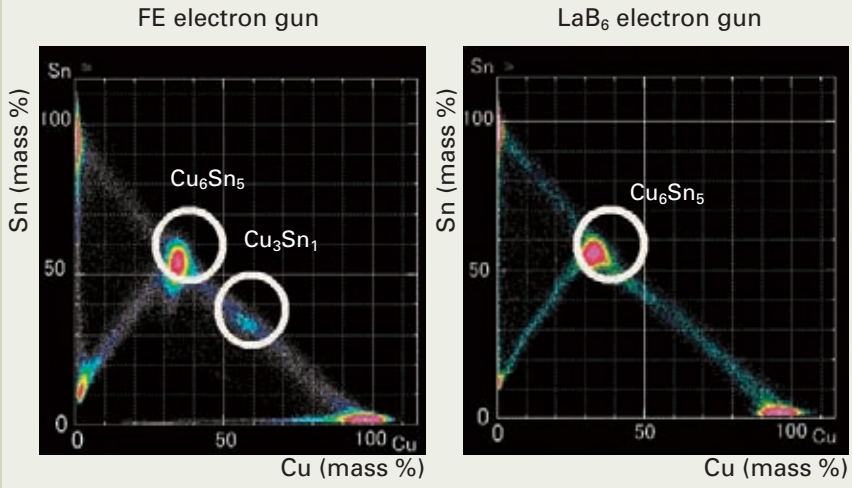

Fig. 14 Phase analysis of Cu-solder interface by FE and LaB_6 guns. The FE gun was able to detect the presence of a Cu_3Sn_1 alloy layer. See attached color images.